Annual impact of wind-farm gravity waves on the Belgian–Dutch offshore wind-farm cluster

IOP Conf. Series: Journal of Physics: Conf. Series **1037** (2018) 072006 doi:10.1088/1742-6596/1037/7/072006

Annual impact of wind-farm gravity waves on the Belgian–Dutch offshore wind-farm cluster

Dries Allaerts[1], Sam Vanden Broucke[2], Nicole van Lipzig[2] and Johan Meyers[1]

[1] KU Leuven, Department of Mechanical Engineering, Celestijnenlaan 300 – box 2421, B-3001 Leuven, Belgium

[2] KU Leuven, Department of Earth and Environmental Sciences, Celestijnenlaan 200E – box 2409, B-3001 Leuven, Belgium

E-mail: dries.allaerts@kuleuven.be

Abstract. While research on wind-farm–atmospheric boundary layer interaction has primarily focused on local effects inside and above the farm, recent studies found that wind farms may affect the wind conditions several kilometres upstream of the farm via the excitation of atmospheric gravity waves. Such non-local effects can have strong implications for the wind-farm energy extraction but are currently overlooked in wind-farm design and operation and control strategies. In the present study, we employ a fast wind-farm boundary-layer model in combination with ERA5 reanalysis data to assess the potential impact of wind-farm induced gravity waves on the annual energy production of the Belgian–Dutch offshore wind-farm cluster in the North Sea. We estimate the annual energy loss due to the effect of self-induced gravity waves to be of the order of 4 to 6 %.

1. Introduction

Over the past years, research on the interaction between wind farms and the atmospheric boundary layer has primarily focused on local effects related to the complex interaction of multiple turbine wakes and the associated slow down of the atmosphere inside and above the farm; see Ref. [1] for a review. However, recent large-eddy simulation (LES) studies showed that the upward flow displacement in response to the collective flow blockage in large wind farms may excite atmospheric gravity waves on overlying inversion layers and in the free atmosphere [2, 3, 4]. These gravity waves impose significant pressure gradients in the boundary layer and may lead to modified wind conditions several kilometres upstream of the farm. Such non-local effects are currently overlooked in the design of new wind farms and in the development of operation and control strategies, i.e., the wind-energy community consistently assumes that the wind speed at the upwind edge of a wind-turbine array is not affected and can be taken from prior measurement campaigns or wind-atlas data. In reality, upstream wind speeds may be considerably lower under operational conditions, resulting in reduced wind-farm power output.

The purpose of this study is to assess the potential impact of atmospheric gravity waves and upstream flow deceleration on the annual energy production (AEP) of a realistic wind farm. However, using LES to perform AEP estimations including gravity-wave effects is currently infeasible on state-of-the-art high-performance computing infrastructure, so a fast wind-farm boundary-layer model is required. Since non-local effects are systematically neglected in wake

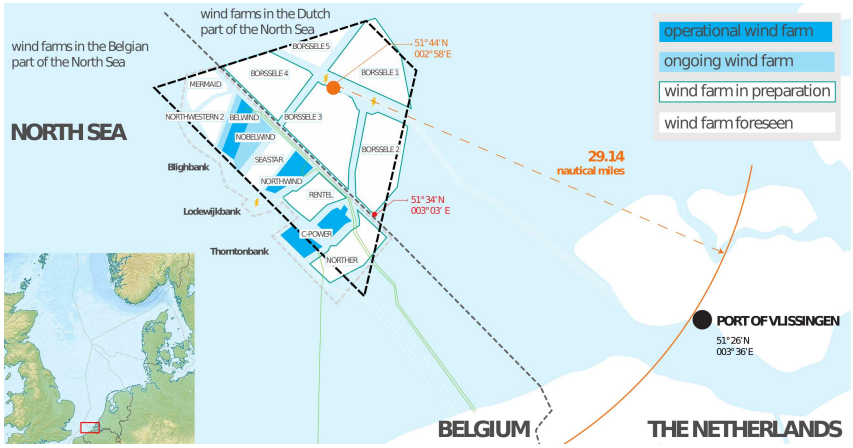

Figure 1. Offshore wind farms in the Belgian and Dutch part of the North Sea. The dashed lines indicate the simplified shape used in the current study. Figure adapted from Ref. [8]

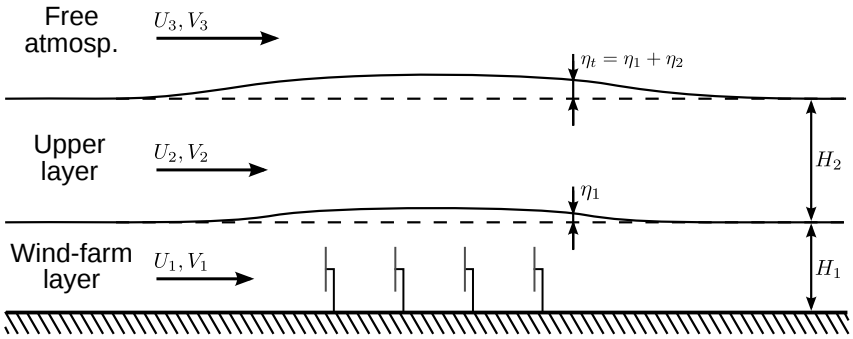

Figure 2. Computational set-up of the three-layer model.

models available in literature, we employ a new model based on a three-layer representation of the atmosphere, designed for the specific purpose of investigating wind-farm induced gravity waves. The three-layer model is an extension of the linear gravity-wave theory used to study atmospheric disturbances caused by mountains or wind farms [5, 6, 7], and it accounts for feedback effects on wind-farm drag and energy extraction. A one-dimensional variant of the model (with two layers) has been used before to analyse the impact of nocturnal low-level jets on gravity-wave excitation [4].

In the current study, we focus on a large wind-farm cluster in the North Sea, comprised of the entire Belgian offshore wind-farm zone and the adjacent Borssele wind-farm zone located in the Exclusive Economic Zone of the Netherlands (see figure 1). In the Belgian North Sea, a zone of 238 km^2 is reserved for wind energy development and 9 projects have been granted permission to build and operate wind farms. The Borssele zone, on the other hand, is approximately 344 km^2 and is sub-divided into 5 wind-farm sites. Together, these projects constitute a wind-farm cluster of 582 km^2 with a planned capacity of 3,680 – 3,800 MW fully commissioned by the end of 2020.

The potential impact of gravity waves on the AEP of the Belgian–Dutch offshore wind-farm cluster is assessed based on three-layer model simulations driven by ERA5 reanalysis data of the year 2016. A brief description of the three-layer model is provided in section 2. In section 3, we describe how atmospheric model parameters are extracted from the reanalysis data. The results are presented in section 4 and conclusion are drawn in section 5.

2. Three-layer model

The idea of the three-layer model is to divide the vertical structure of the atmosphere into three parts (see figure 2). The lowest layer represents the region where the drag of the wind turbines is directly felt. The second layer lies above the wind-farm layer and extends up to the capping

inversion. The free atmosphere above the inversion constitutes the third layer of the model. We describe the governing flow equations for the three layers in § 2.1 and discuss the wind-farm configuration in § 2.2. The validation of the model is summarised in § 2.3.

2.1. Flow model

The two layers below the inversion are modelled explicitly with two-dimensional depth-averaged linearised flow equations:

$$U_{j,1}\frac{\partial u_{i,1}}{\partial x_j} + \frac{1}{\rho_0}\frac{\partial p}{\partial x_i} = f_c\epsilon_{ij3}u_{j,1} + \frac{D'_{ij}}{H_1}\Delta_1^2 u_j - \frac{C'_{ij}}{H_1}u_{j,1} - \frac{f_i^{(0)} + f_i^{(1)}}{H_1}, \tag{1}$$

$$U_{j,2}\frac{\partial u_{i,2}}{\partial x_j} + \frac{1}{\rho_0}\frac{\partial p}{\partial x_i} = f_c\epsilon_{ij3}u_{j,2} - \frac{D'_{ij}}{H_2}\Delta_1^2 u_j, \tag{2}$$

$$U_{j,1}\frac{\partial \eta_1}{\partial x_j} + H_1\frac{\partial u_{j,1}}{\partial x_j} = 0, \tag{3}$$

$$U_{j,2}\frac{\partial \eta_2}{\partial x_j} + H_2\frac{\partial u_{j,2}}{\partial x_j} = 0, \tag{4}$$

with i, j equal to $1, 2$. The atmospheric base state is governed by the mean depth-averaged wind speeds $U_{i,1}$ and $U_{i,2}$ (with $i = 1, 2$) and the layer heights H_1 and H_2 of the wind-farm and upper layer, respectively, and $(u_{i,1}, u_{i,2}, \eta_1, \eta_2)$ represent the perturbations to this reference state. Further, $\Delta_1^2 u_j = u_{j,2} - u_{j,1}$ is the difference in velocity perturbation between the wind-farm and upper layer and $f_c = 2\Omega\sin\phi$ is the Coriolis parameter (with Ω the angular velocity of the earth and ϕ the latitude). The matrices C'_{ij} and D'_{ij} describe the perturbation of the friction at the ground and at the interface between both layers, respectively, and they are given by

$$C'_{ij} = \frac{C}{\sqrt{U_{k,1}U_{k,1}}}\left(U_{i,1}U_{j,1} + \delta_{ij}U_{k,1}U_{k,1}\right), \tag{5}$$

$$D'_{ij} = \frac{D}{\sqrt{\Delta_1^2 U_k \Delta_1^2 U_k}}\left(\Delta_1^2 U_i \Delta_1^2 U_j + \delta_{ij}\Delta_1^2 U_k \Delta_1^2 U_k\right), \tag{6}$$

with $\Delta_1^2 U_j = U_{j,2} - U_{j,1}$ the difference in background velocity and C and D the drag coefficients of the unperturbed atmospheric state. Horizontal turbulent diffusion and momentum entrainment at the inversion layer are neglected, and the boundary layer is assumed to be hydrostatic (i.e., the pressure perturbation is constant with height and only depends on the flow conditions in the free atmosphere). The terms $f_i^{(0)}$ and $f_i^{(1)}$ represent the zeroth- and first-order terms of the Taylor expansion of the wind-farm drag f_i, which is further discussed in § 2.2.

The third layer of the model provides a relationship between the pressure and the total vertical displacement $\eta_t = \eta_1 + \eta_2$. Following Ref. [7], an analytical expression can be inferred from linear three-dimensional gravity wave theory (assuming constant wind speed $\boldsymbol{U}_3 = (U_3, V_3)$ and Brunt-Väisälä frequency N). In Fourier components (denoted by a hat), the pressure disturbance at the inversion layer can be related to the vertical displacement as

$$\hat{p}/\rho_0 = \left(g' + \hat{\Phi}\right)\hat{\eta}_t \quad \text{where} \quad \hat{\Phi} = \frac{i\left(N^2 - \Omega^2\right)}{m}. \tag{7}$$

Here, the reduced gravity $g' = g\Delta\theta/\theta_0$ (with $\Delta\theta$ the inversion strength) accounts for waves on the inversion layer, while the effect of internal gravity waves is represented by the complex stratification coefficient $\hat{\Phi}(k, l)$. The intrinsic frequency of internal waves is defined as $\Omega =$

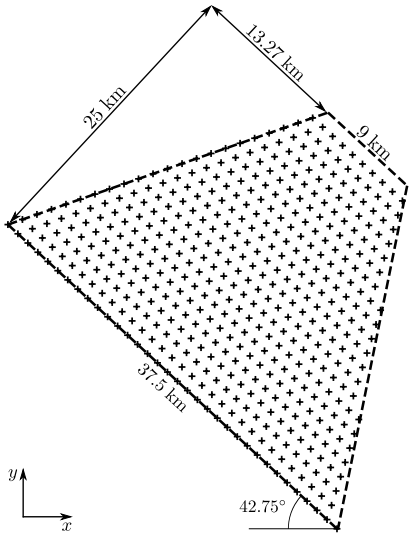

Figure 3. Sketch of the wind-farm model, showing the orientation and dimensions of the trapezoid shape and the turbine layout.

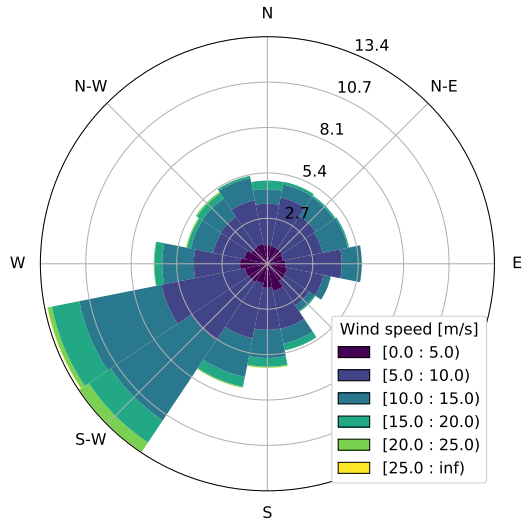

Figure 4. Wind rose plot of the height-averaged winds in the wind-farm layer (U_1, V_1).

$-\boldsymbol{\kappa} \cdot \boldsymbol{U}_3$ with $\boldsymbol{\kappa} = (k, l)$ the horizontal wavenumber vector. The vertical wave number $m(k, l)$ follows from the dispersion relation [9]

$$m^2 = (k^2 + l^2)\left(\frac{N^2}{\Omega^2} - 1\right). \tag{8}$$

The three-layer model is discretised with a Fourier–Galerkin method. The first-order part of the wind-farm drag involves the product of two spatially dependent functions and is calculated in physical space in order to avoid the expensive convolution sum in Fourier space. Aliasing errors are thereby removed using the 3/2-rule [10]. The discretised equations form a linear matrix equation which is solved with the LGMRES algorithm [11]. We use a numerical domain of 1000 by 400 km at a uniform grid resolution of 500 m to allow the perturbations to die out before being recycled by the periodic boundary conditions.

2.2. Wind-farm model

For simplicity, we represent the Belgian–Dutch wind-farm cluster as a trapezoidal shape with a surface area of 582 km^2 (see figures 1 and 3). Moreover, we assume that all wind farms are equipped with the same 8 MW wind turbine and that a total of 475 turbines are installed equidistantly in the wind-farm zone in a staggered pattern with respect to the dominant inflow direction (cf. figures 3 and 4). We consider turbines with a constant thrust coefficient $C_T = 0.8$, a rotor diameter of 154 m and a turbine hub height $z_h = 120$ m.

The drag exerted by this wind-turbine array on the flow is represented by an external force f_i in the depth-averaged momentum equation for the wind-farm layer. In order to account for turbine wake interactions, we employ the Gaussian wake model [12] to compute the thrust forces $\boldsymbol{f}_k = (f_{i,k})$ of the individual wind turbines $k = 1, \ldots, N_t$. In addition to turbine dimensions and locations, input for the wake model includes the free-stream velocity $\boldsymbol{u}_{\mathrm{fs}}$ upstream of the first turbine (i.e., the velocity measured upstream before local pressure build up in front of the turbine slows down the approaching flow) and the ambient turbulent intensity I_0 at hub height.

Linearisation of the wake model relies on the Taylor expansion of the thrust force $\boldsymbol{f}_k$ about the unperturbed inflow velocity $\overline{\boldsymbol{u}}_{\text{fs}}$, given by

$$\boldsymbol{f}_k(\boldsymbol{u}_{\text{fs}}) = \boldsymbol{f}_k(\overline{\boldsymbol{u}}_{\text{fs}}) + \boldsymbol{J}^k_{\boldsymbol{f}}(\overline{\boldsymbol{u}}_{\text{fs}})\,(\boldsymbol{u}_{\text{fs}} - \overline{\boldsymbol{u}}_{\text{fs}}) + O(\|\boldsymbol{u}_{\text{fs}} - \overline{\boldsymbol{u}}_{\text{fs}}\|^2), \tag{9}$$

with $\boldsymbol{J}^k_{\boldsymbol{f}}$ the Jacobian of the wake model. The unperturbed inflow velocity $\overline{\boldsymbol{u}}_{\text{fs}}$ is equal to the mean wind speed (U_1, V_1) in the wind-farm layer, and the perturbation velocity $\boldsymbol{u}_{\text{fs}} - \overline{\boldsymbol{u}}_{\text{fs}} = (u_1, v_1)$ is taken $10D$ upstream of the first wind turbine. Further, we assume that the upstream turbulent intensity is not affected by gravity wave effects.

The turbine forces computed with the Gaussian wake model are filtered on the numerical grid of the three-layer model using a Gaussian filter:

$$f_i(x,y) = \int_0^{L_x}\int_0^{L_y} G(x-x', y-y') \sum_k^{N_t} f_{i,k}\delta(x'-x_k, y'-y_k)\,\mathrm{d}x'\,\mathrm{d}y', \tag{10}$$

with $L_x \times L_y$ the size of the domain, (x_k, y_k) the location of turbine k and $G(x,y)$ the 2D Gaussian kernel

$$G(x,y) = \frac{1}{\pi L^2}\exp\left(-\frac{x^2+y^2}{L^2}\right). \tag{11}$$

We set the filter length $L = 1$ km.

2.3. Model validation

We present the results of a validation study with LES data from Refs. [2, 4]. Since these LES studies consider "infinitely" wide wind farms, the LES data can only be used to validate a one-dimensional version of the three-layer model. The validation is performed using a numerical domain of 1000 km at a grid resolution of 300 m. We also compare the performance of the three-layer model with the model developed in Ref. [7], which is comprised of only two layers, i.e., the boundary layer and the free atmosphere.

Figure 5 gives a global overview of the model performance by comparing model predictions and LES results of two metrics: the maximum displacement of the inversion layer relative to the undisturbed inversion height and the relative velocity reduction averaged over the farm area. It is shown that the three-layer model predictions of inversion layer displacement are relatively close to the LES results (within 5 percentage points (pp), mean absolute error is 0.9 pp). The prediction of the relative velocity reduction is good at low perturbation values, but the model tends to underestimate the velocity reduction with increasing perturbation values (maximum difference of 11 pp, mean absolute error is 5 pp), which is attributed to non-linear effects. Further, it is shown that the three-layer model outperforms the simple two-layer model, which often overpredicts the inversion-layer displacement and performs poorly in terms of relative velocity reduction. We conclude that the three-layer model performs reasonably well and can be used to obtain a conservative estimate of gravity-wave induced effects. A more elaborate validation study focusing on various aspects of the three-layer model is subject to further research.

3. Atmospheric conditions

The background atmospheric state of the three-layer model is deduced from ERA5 reanalysis data of the year 2016, which is available at hourly frequency. Data processing for ERA5 is carried out by ECMWF, using ECMWF's Earth System model IFS, cycle 41r2. The acronym ERA refers to *ECMWF ReAnalysis*, with ERA5 being the fifth major global reanalysis produced by ECMWF (after FGGE, ERA-15, ERA-40 and ERA-Interim). We use surface data and vertical profiles from the grid point nearest to the wind-farm cluster, located at 51.6N 3.0E.

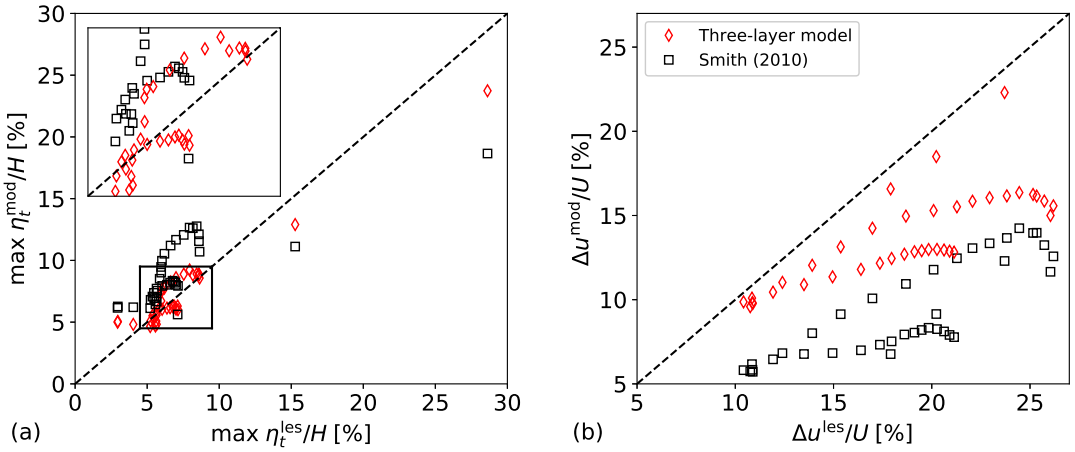

Figure 5. Predictions obtained with the three-layer model and a simpler two-layer model [7] versus LES results for various cases, showing (a) maximum displacement of the inversion layer relative to the undisturbed inversion height and (b) relative velocity reduction averaged over the farm area.

The atmospheric state is determined as follows. First, we fit a smooth analytical curve to the vertical profile of virtual potential temperature (ignoring any temperature variations in the surface layer) [13]. As inversion waves will only exist for very shallow capping inversions, we require that the inversion depth $\Delta h \leq 300$ m in the fitting problem. The outcome of this procedure is an estimate of the strength $\Delta\theta$, depth Δh and height h_1 of the inversion layer and the Brunt-Väisälä frequency N in the free atmosphere. The height of the upper layer H_2 is then set such that $H_1 + H_2 = h_1$, with the wind-farm layer height chosen to be $H_1 = 2z_h$. Next, the velocities (U_1, V_1) and (U_2, V_2) are obtained by vertically averaging the velocity profiles in the wind-farm and upper layer. The velocity of the free atmosphere (U_3, V_3) is set equal to the velocity at $h_1 + \Delta h/2$. The ERA5 data-set does not contain vertical profiles of shear stress, so we parametrise these as

$$\tau(z) = \begin{cases} u_*^2 \left(1 - z/h_{\mathrm{bl}}\right)^{\beta} & z \leq h_{\mathrm{bl}} \\ 0 & z > h_{\mathrm{bl}} \end{cases} \tag{12}$$

with u_* the surface friction velocity and h_{bl} the height of the turbulent boundary layer. For neutral and convective boundary layers, we take $h_{\mathrm{bl}} = h_1$ and set $\beta = 1.0$ [14]. For stable boundary layers, we set $\beta = 1.5$ [15] and employ the ERA5 prediction of the boundary-layer height for h_{bl}. This height may be lower than h_1 when a residual layer exists between the stable boundary layer and the inversion layer. With these shear stress profiles, the friction coefficients are computed as

$$C = \frac{\tau[z=0]}{U_{k,1}U_{k,1}} \quad \text{and} \quad D = \frac{\tau[z=H_1]}{\Delta_1^2 U_k \Delta_1^2 U_k}. \tag{13}$$

The distribution of the height-averaged wind speed and direction in the wind-farm layer is illustrated in figure 4. It shows that the dominant wind directions are southwest and west-southwest with a probability of 13.4 % and 13.3 %, respectively. Further, we find that the height-averaged wind speed is less than 10 m/s in about 63.8 % of year and rarely exceeds 20 m/s.

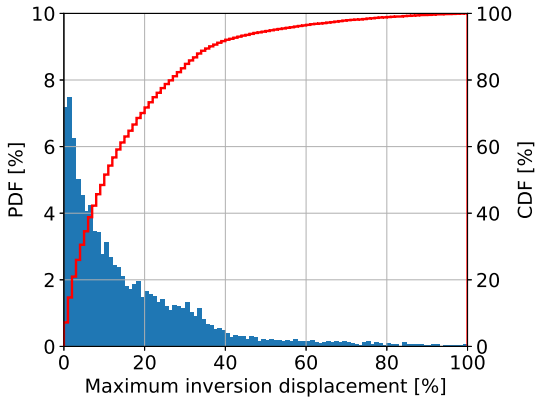

Figure 6. Probability density function and cumulative density function of the maximum inversion layer displacement (relative to the undisturbed inversion height).

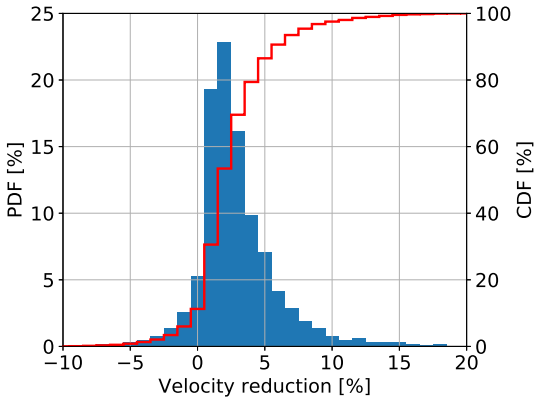

Figure 7. Probability density function and cumulative density function of the relative velocity reduction in front of the wind farm (measured $10D$ upstream of the first turbine).

4. Results and discussion

We perform 8784 independent simulations with the three-layer model (one for every hour of 2016) and present the results by means of the probability and cumulative density functions. Figure 6 shows the distribution of the maximum inversion-layer displacement, which is a proxy for the amplitude of the gravity waves excited by the wind-farm cluster. We find that the inversion-layer displacement is almost always significant and that it is even higher than 10 % of the undisturbed inversion height in more than 50 % of the cases.

The distribution of the relative velocity reduction upstream of the wind-farm cluster is shown in figure 7. In about 75 % of the cases, the upstream wind decelerates between 0 and 5 % due to a counteracting pressure gradient induced by atmospheric gravity waves. The velocity reduction is higher under certain atmospheric conditions, but it is rarely more than 10 %. We also find some cases with a negative velocity reduction, indicating that the wind is in fact accelerating in front of the farm. However, it is not clear whether these are realistic physical conditions or numerical artefacts caused by the recycling of gravity wave perturbations by the periodic boundary conditions.

Figure 8 shows the distribution of the power loss related to gravity-wave effects, calculated with respect to the power output of the same wind farm (so including wake effects) in the absence of gravity waves. We find that the power loss ranges between 0 and 10 % in 58.7 % of the cases. Further, the power appears to increase instead of decrease in about 10 % of the cases due to upstream flow acceleration. Integrated over the entire year, we find that the annual energy production of the Belgian–Dutch offshore wind-farm cluster will be 6.47 % lower due to the effect of self-induced gravity waves.

In order to put this value into perspective, we run several AEP simulations with different model assumptions and assess the model uncertainty (see table 1). An import source of uncertainty is the simplified representation of the vertical structure of the atmosphere and the difficulty to extract model parameters from continuous vertical profiles. For instance, we assume a constant velocity in the free atmosphere, while in reality baroclinicity or non-stationary synoptic conditions may result in considerable velocity variations above the inversion layer. To asses how our definition of free atmosphere velocity $\boldsymbol{U}_3$ affects the results, we run an AEP simulations in which $\boldsymbol{U}_3$ is obtained by averaging the velocity between h_1 and 5000 m (instead

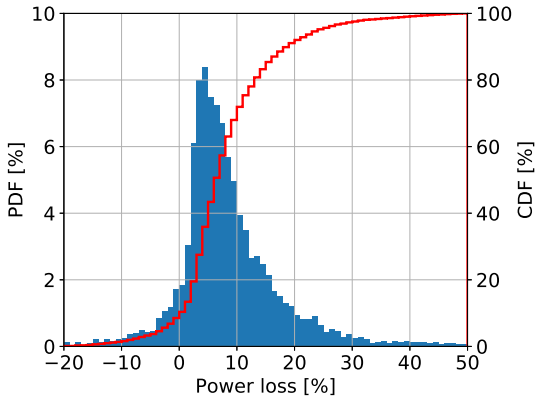

Figure 8. Probability density function and cumulative density function of the power loss due to gravity wave effects.

Table 1. Impact of various model assumptions on the prediction of annual energy loss caused by atmospheric gravity waves.

Description	Annual energy loss [%]
Baseline case	6.47
Free atmosphere velocity $\boldsymbol{U}_3$ averaged between h_1 and 5000 m	4.84
Inversion depth constraint $\Delta h_{\max} = 3000$ m	6.83
Without inversion waves	3.84
Reanalysis data at 51.6N 2.7E	6.36

of taking the value at $h_1 + \Delta h/2$). The annual energy loss is lower for this case (4.84 compared to 6.47 %), yet the order of magnitude is the same. Further, the model does not account for non-uniform stratification in the free atmosphere, and the curve fitting procedure may not always correctly identify the presence or absence of inversion layers. We checked the impact of the constraint on the inversion depth by setting $\Delta h_{\max} = 3000$ m instead of 300 m, but the annual energy loss changes only very little. Even when we completely ignore capping inversions and associated inversion waves, we find that the annual energy loss is still of the order of 4 %. Finally, we investigate whether the choice of ERA5 grid point makes a difference, but choosing a grid point farther offshore does not change the results significantly.

5. Conclusion

The aim of the current study was to assess the annual impact of wind-farm gravity waves on the Belgian–Dutch wind-farm cluster in the North Sea. Although large-eddy simulations had been used before to study wind-farm gravity waves under specific conditions, using LES to perform the envisaged AEP simulations was numerically not feasible. Therefore, we relied on a fast wind-farm boundary-layer model that was designed for the specific purpose of investigating gravity wave feedback effects. In this model, the vertical structure of the atmosphere is represented with three layers, and we used ERA5 reanalysis data of the year 2016 to specify the model parameters.

Based on several AEP simulations with varying model assumptions, we conclude that the annual energy loss of the fully operational Belgian–Dutch offshore wind-farm cluster due to self-induced gravity waves could be of the order of 4 to 6 %. The uncertainty on this figure mainly comes from the simplified vertical structure of the model and the difficulty to extract model parameters from continuous vertical profiles. First, we noticed that the definition of the free

atmosphere wind speed has considerable impact on the predicted annual energy loss. Therefore, more research is required to quantify the effect of baroclinicity on wind-farm gravity waves. Further, we encountered several cases in which the atmosphere's vertical structure is very hard to represent with the three-layer model, e.g., cases with multiple inversion layers, non-uniform stratification of the free atmosphere and extremely shallow boundary layers. Adapting the model to be able to distinguish between these different flow cases could improve the reliability of the model and would be an interesting topic for further research. Finally, we stress that the current AEP predictions are based on the assumption of a constant thrust coefficient and could be improved by considering the actual power curve as a function of wind speed.

Acknowledgments
The computational resources and services used in this work were provided by the VSC (Flemish Supercomputer Center), funded by the Research Foundation Flanders (FWO) and the Flemish Government – department EWI.

References

[1] Stevens R J A M and Meneveau C 2017 *Annu. Rev. Fluid Mech.* **49** 311–339
[2] Allaerts D and Meyers J 2017 *J. Fluid Mech.* **814** 95–130
[3] Wu K L and Porté-Agel F 2017 *Energies* **10** 2164
[4] Allaerts D and Meyers J 2018 *Boundary-Layer Meteorol.* **166** 269–299
[5] Smith R B, Jiang Q and Doyle J D 2006 *J. Atmos. Sci.* **63** 774–781
[6] Smith R B 2007 *J. Atmos. Sci.* **64** 594–607
[7] Smith R B 2010 *Wind Energy* **13** 449–458 ISSN 1099-1824
[8] Renewabel Energy Base Oostende (REBO) 2016 General folder URL `https://www.reboostende.be`
[9] Smith R B 1980 *Tellus* **32** 348–364 ISSN 2153-3490
[10] Canuto C, Hussaini M Y, Quarteroni A and Zang T A 1988 *Spectral Methods in Fluid Dynamics* (Springer-Verlag, Berlin)
[11] Baker A H, Jessup E R and Manteuffel T 2005 *SIAM J. Matrix Anal. & Appl.* **26** 962–984
[12] Niayifar A and Porté-Agel F 2016 *Energies* **9** 741
[13] Rampanelli G and Zardi D 2004 *J. Appl. Meteor.* **43** 925–933 ISSN 0894-8763
[14] Stull R B 1988 *An Introduction to Boundary Layer Meteorology* (Springer)
[15] Nieuwstadt F T M 1984 *J. Atmos. Sci.* **41** 2202–2216